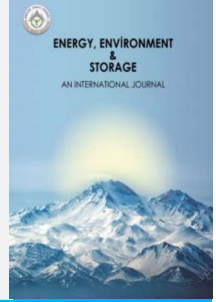




Energy, Environment and Storage

Journal Homepage: www.enenstrg.com



Numerical and Optimization Study on a Heat Exchanger Tube Inserted with Ring by Taguchi Approach

Toygun Dagdevir^{1*},

¹Erciyes University, Dept. of Mechanical Engineering, Kayseri, Turkey, ORCID: 0000-0001-7388-3391

ABSTRACT. This paper presents an optimization study on a heat exchanger tube inserted with circular rings by using numerical analysis results. Pitch length (50, 100 and 200 mm), inner diameter (15, 12.5 and 10.0 mm) and thickness (1, 3 and 5 mm) of the rings are considered as factors to be optimized. Water is selected as working fluid and the tube is considered under constant heat flux of 20 kW/m² and turbulent flow condition. k-ε RNG turbulent model is used to simulate the turbulent flow through the tube. L9 design of experiment model is used to reduce the number of numerical runs which is proposed by Taguchi method. The optimization study is conducted as single and multi objective optimization by using Taguchi method and Grey relation analysis. Furthermore, the contribution effects of the considered parameters on the Nusselt number and the friction factor result are revealed by ANOVA. Numerical results showed that the Nusselt number and the friction factor increases as the pitch length, the diameter and the thickness decreases. It is found that the most effective parameters on both the Nusselt number and the friction factor is inner diameter of the rings. For the single-objective optimization, the highest Nusselt number and the lowest friction factor is obtained with the tube configuration that are found as the pitch length of 50 mm, the diameter of 10 mm and the thickness of 5 mm and the pitch length of 200 mm, the diameter of 15 mm and the thickness of 3.0 mm, respectively. The pitch length of 50 mm, the diameter of 15.0 mm and the thickness of 5.0 mm presents the best thermal and hydraulic performance according to the multi-objective optimization study.

Keywords: Heat transfer enhancement, Taguchi method, Grey relation analysis, ring inserted tube, computational fluid dynamics

Article History: Received:28.12.2022; Accepted:06.01.2023; Available Online:25.01.2023

Doi: <https://doi.org/10.52924/OQGS5091>

1. INTRODUCTION

Increasing in population, depleting the fossil fuel sources and improvements on technology cause to increase in energy demand and cost. Therefore, the efficient use of energy has become inevitable. Since heat energy is the most irreversible energy type, heat transfer enhancement studies are popular and necessary. Heat transfer enhancement techniques are classified in two groups such as active and passive[1]. Active techniques require extra power input to the system, while passive techniques are based on the physical modification on the system[2]. The active techniques are not widely preferred due to having complexity, weight and control system, although they are successful in heat transfer. Therefore, the passive techniques are more preferred due to its advantageousness compared to the active techniques [3].

The most popular passive methods are coiled tubes [4], extended surfaces [5], rough surfaces [6], swirl flow devices (twisted tape) [7], conical ring [8], vortex rings [6] and coiled wire [9] etc. The common conclusion from the techniques applied for heat transfer enhancement increases not only Nusselt number (Nu), but also friction factor (f).

These two results are evaluated according to thermo-hydraulic performance criteria (THP) in literature. The THP value greater than 1.0 indicates that the applied technique is suitable for both thermal and hydraulic performance in practice.

Promvonge [10] investigated that the performance of conical rings for passive heat enhancement technique. They resulted that the enhancement in Nusselt number is achieved up to 197%, 333% and 237% for the use of CR, DR and CDR, respectively. They also reported correlations for the Nu and the f results belongs to conical ring used heat exchanger tube.

$$Nu = 0.09155Re^{0.655}Pr^{0.4} \left(\frac{d}{D}\right)^{-1.31} \quad (1)$$

$$f = 1.12Re^{-0.258} \left(\frac{d}{D}\right)^{-4.4} \quad (2)$$

Promvonge and Eiamsa-ard [11] also investigated the effect of conical-nozzle turbulators on heat transfer and turbulent flow in a circular tube. Heat transfer, friction

* Corresponding author: toygun@erciyes.edu.tr

factor and thermo-hydraulic performance of a circular tube fitted with conical-ring and twisted tape inserts is experimentally investigated by Promvongse and Eiamsaard [12]. They found that the THP tends to decrease for using all conical-ring and twisted tape insert cases with the increment of Reynolds number. Kongkaiatpaiboon et al. [13] investigated the perforated conical-ring on heat transfer enhancement. They found that the heat transfer rate and friction factor increase with decreasing number of perforated holes, pitch ratio. In addition to thermal and hydraulic performance researches, the cooling/heating systems need an optimum configuration including heat transfer enhancement technique. Majid et al. [14] conducted a research on optimization of heat transfer on helically coiled pipe flowing nanofluid using Taguchi method. Poornodoya et al. [15] optimized the performance parameters of a double pipe heat exchanger with cut twisted tape using respond surface method. Turgut et al. [16] researched the optimization of the concentric heat exchanger with injector turbulators by Taguchi method. Chamoli et al. [17] applied Taguchi method on flow and geometrical parameters in a rectangular channel roughened with down perforated baffles. Dagdevir [18] optimized the dimpled heat exchanger tube parameters according to multi-objective parameters such as the Nu and the f .

Since Taguchi method has a great advantageous with design of experiment which significantly reduce the number of the experimental or numerical runs [19], many researchers used the method to optimize their results.

According to the literature review, the passive heat transfer enhancement techniques promise to design better, lower size, energy saver heat exchangers, and Taguchi method is useful for optimizing the results and reduce the runs. It is recognized that there is a gap in the literature about optimization of circular tube fitted with circular ring on thermal and hydraulic performance. Therefore, it is focused on researching the thermal and hydraulic results and optimizing the parameters of a circular heat exchanger tube fitted with various rings arrays and dimensions in the present study.

2. MATERIALS AND METHODS

2.1 Numerical method

In order to investigate and optimize the circular tube inserted with rings, a solution domain is modeled as depicted in Fig. 1. The solution domain composes of three sections: entrance section, test section and exit section with lengths of 200 mm, 1000 mm and 100 mm, respectively. Inner diameter of the tube (D) is selected as 17.272 mm. The results are considered for the test section; however, the entrance section and the exit section should be created for the insurances of the numerical procedure. On a hand, the test section is created to provide fully developed flow with a length at least ten times diameter of the tube, as suggested by Incropera et al. [20]. On the other hand, the exit section is created to prevent reverse flow error which is not normal to pressure outlet surface by rings.

In order to model a heat exchanger tube, a constant heat flux boundary condition is applied on the test section as 20 kW/m². Wall boundary conditions is assumed as no slip for entire sections. Inlet of the tube is assumed as velocity inlet and it is calculated according to Reynolds number. The outlet of the tube is selected as pressure outlet with gauge pressure of 0 Pa to simulate atmospheric condition.

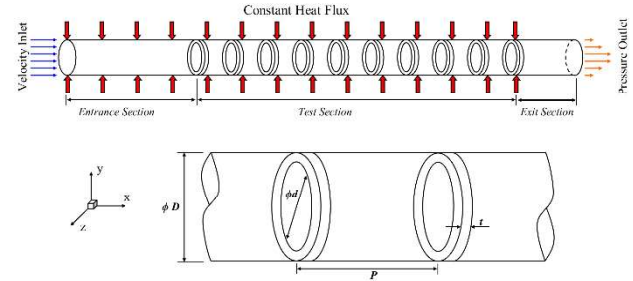


Fig. 1. Schematical view of the solution domain

2.2 Governing equations

This study is conducted by employing the CFD software, Fluent version 18.0, which solves governing conservation equations with finite volume technique. The equations at steady state conditions are given as below [21]:

Mass conservation equation:

$$\nabla(\rho\vec{V}) = 0 \quad (3)$$

Momentum conservation equation:

$$\nabla(\rho\vec{V}\vec{V}) = -\nabla P + \nabla(\mu\vec{\nabla}\vec{V}) \quad (4)$$

Energy conservation equation:

$$\nabla(\rho c_p \vec{V}T) = \nabla(k\nabla T) \quad (5)$$

where ρ is fluid density, V is velocity, P is pressure, μ is dynamic viscosity, c_p is specific heat capacity, k is thermal conductivity, and T is temperature. RNG turbulence model is adopted for the all cases. The RNG transport equation for kinetic energy k and ε turbulence dissipation:

$$\frac{\partial}{\partial t}(\rho k) + \frac{\partial}{\partial x_i}(\rho k u_i) = \frac{\partial}{\partial x_j}(\alpha_k \mu_{eff} \frac{\partial k}{\partial x_j}) + G_k + G_b - \rho \varepsilon - Y_m + S_k \quad (6)$$

$$\frac{\partial}{\partial t}(\rho \varepsilon) + \frac{\partial}{\partial x_i}(\rho \varepsilon u_i) = \frac{\partial}{\partial x_j}(\alpha_\varepsilon \mu_{eff} \frac{\partial \varepsilon}{\partial x_j}) + C_{1\varepsilon} \frac{\varepsilon}{k} (G_k + C_{3\varepsilon} G_b) - C_{2\varepsilon} \rho \frac{\varepsilon^2}{k} - R_\varepsilon + S_\varepsilon \quad (7)$$

In these equations, G_k represents the generation of turbulence kinetic energy due to the mean velocity gradients. G_b is the generation of turbulence kinetic energy due to buoyancy. Y_m represents the contribution of the fluctuating dilatation in compressible turbulence to the overall dissipation rate. The quantities α_k and α_ε are the inverse effective Prandtl numbers for k and respectively. S_k and S_ε are user-defined source terms. Detail information is available in Fluent Theory Guide [21].

$$C_2^* = C_{2\epsilon} + \frac{C_{\mu}\eta^3(1-\eta/\eta_0)}{1+\beta\eta^3} \quad (8)$$

$$\eta = Sk/\epsilon S = (2S_{ij}S_{ij})^{1/2} \quad (9)$$

Used constants of the turbulence model are given as below:

$$C_{\mu} = 0.0845, \sigma_k = 0.7194, \sigma_{\epsilon} = 0.7194, \\ C_{\epsilon 1} = 1.42, C_{\epsilon 2} = 1.68, \eta_0 = 4.38, \beta = 0.012 \quad (10)$$

Semi Implicit Method for Pressure Linked Equations (SIMPLE) algorithm scheme is conducted to achieve the relationship between pressure and velocity coupling to enforce mass conservation and to obtain pressure field [21]. Quadratic Upstream Interpolation for Convective Kinematics (QUICK) scheme is used for discretion of convection terms and diffusion terms. The residual criteria of continuity, velocities, energy, k and ϵ are taken as 1×10^{-5} to ensure convergence of the solution.

2.3 Data reduction

Used data are exported from the software with area-weighted average by using surface integral. The Reynolds number (Re), which is ratio of inertial force to viscous force, is expressed as:

$$Re = \frac{\rho DV}{\mu} \quad (11)$$

where ρ density of the fluid, D is diameter of the tube, V velocity of the fluid and μ is dynamic viscosity of the fluid.

The average Nusselt number (\overline{Nu}), which is ratio of convective heat transfer rate to conductive heat transfer rate, is expressed as:

$$\overline{Nu} = \frac{\overline{h}D}{k} \quad (12)$$

k is thermal conductivity of the fluid, and the average convective heat transfer coefficient (\overline{h}) along the test section is calculated as:

$$\overline{h} = \frac{q''}{\Delta T} \quad (13)$$

q'' is constant heat flux applied onto the wall surface of the entrance and test section. The average temperature difference (ΔT) in this equation is expressed as:

$$\Delta T = T_s - T_b \quad (14)$$

where T_s is wall surface of the test section temperature and T_b is the fluid bulk temperature between inlet and outlet of the test section.

The friction factor (f) is expressed as:

$$f = \frac{\Delta P}{\frac{1}{2}\rho V^2 \frac{L_{test}}{D}} \quad (15)$$

where ΔP is the pressure difference between inlet and outlet along the test section. L is the length of the test section of the tube.

2.4. Optimization study

The adopted optimization method is used as a paper published by author [18]. Taguchi method is a well-known and beneficial optimization tool due to providing minimum number of experiments determining the best choices of factors affecting the output responses. Because Taguchi method presents only single-objective optimization, Grey relation analysis is applied for a multi-objective optimization. Furthermore, relative contribution effects of the optimized parameters on the output are investigated with using Analysis of variance (ANOVA). Followed steps of the present study are given as the flow chart in Figure 2.

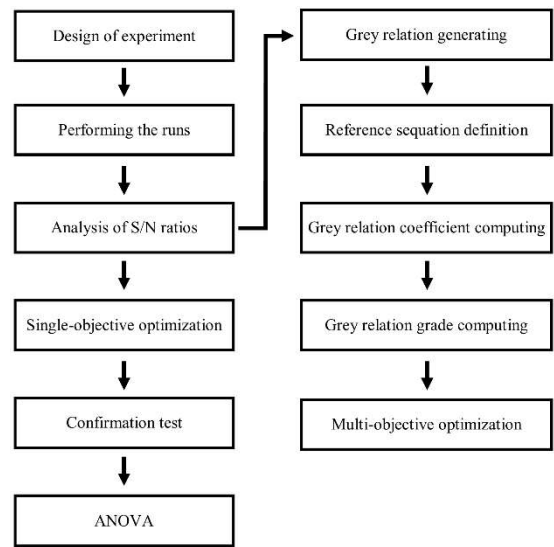


Fig 2. Flow chart of the followed step in the Taguchi method based Grey relation analysis

2.4.1. Design of experiments (DoE)

Taguchi method employs orthogonal arrays to ensure a broad performance of full-factorial experiment [22]. These orthogonal suggests a specific course of action of fragmentary analysis of the influencing parameters and their levels [17]. In this way, time and cost are significantly saved by reducing the number of experiments. The number of required experiment (L_n) is determined with Eq. (16) by the Taguchi method [23]. N_v and N_m represent the number of the variables and the number of maximum levels, respectively.

$$L_n = 1 + N_v[N_m - 1] \quad (16)$$

Table 1 Factors and levels used in the study

| Factors | Levels |
|---------|--------|
|---------|--------|

| | | | |
|-----------------------------------|----------|----------|----------|
| | 1 | 2 | 3 |
| Pitch length of rings (P) [mm] | 50 | 100 | 200 |
| Diameter of rings(d) [mm] | 15.0 | 12.5 | 10.0 |
| Thickness of rings (t) [mm] | 1.0 | 3.0 | 5.0 |

These orthogonal arrays prescribe specific arrangement of fractional experiments with regard to the influencing factors and their levels. The present study adopts L9orthogonal array including 3 factors with 3 levels given in Table 1. Thanks to the advantageous of the Taguchi method, the experiment number is reduced from 27 to 9. The design of experiments (DoE) according to L9 orthogonal array is given in Table 2.

Table 2 Plan for numerical runs

| Runs no. | P | d | t |
|----------|---|---|---|
| 1 | 1 | 1 | 1 |
| 2 | 1 | 2 | 2 |
| 3 | 1 | 3 | 3 |
| 4 | 2 | 1 | 2 |
| 5 | 2 | 2 | 3 |
| 6 | 2 | 3 | 1 |
| 7 | 3 | 1 | 3 |
| 8 | 3 | 2 | 1 |
| 9 | 3 | 3 | 2 |

2.4.2. Signal to Noise ratio

The signal to noise ratios (SNR), denoting with η , of the experiments are obtained from the Taguchi method. The highest SNR value indicates the best level of the parameter. Since the purpose of the study is to determine the highest Nu and the lowest f , functions of “the larger is better” (Eq. (17)) and “the smaller is better” (Eq. (18)) are selected for the Nu and the f , respectively.

$$\eta = -10 \log \left(\frac{1}{n} \sum_{i=1}^n \frac{1}{Y_i^2} \right) \tag{17}$$

$$\eta = -10 \log \left(\frac{1}{n} \sum_{i=1}^n Y_i^2 \right) \tag{18}$$

2.4.3. ANOVA

Furthermore, analysis of variance (ANOVA) is carried out to evaluate the relative contribution effects of the parameters on the Nu and the f . ANOVA uses SNR data obtained from the Taguchi method. In this study, confidence level of the statistical analysis is selected as 95%. F-test is performed to ensure statistically reliability of the procedure. The relevant parameter is statistically significant, if the calculated F-test value is higher than F value. Used equations of the ANOVA are given in from Eq. (19) to Eq. (25).

$$SS_m = \frac{(\sum \eta_i)^2}{j} \tag{19}$$

$$SS_T = \sum \eta_i^2 - SS_m \tag{20}$$

$$SS_A = \frac{(\sum \eta_{Ai})^2}{N} - SS_m \tag{21}$$

$$SS_E = SS_T - \sum SS_A \tag{22}$$

$$V_A = \frac{SS_A}{dof_A} \tag{23}$$

$$dof_A = n_A - 1 \tag{24}$$

$$F_{A0} = \frac{V_A}{V_E} \tag{25}$$

2.4.4. Grey relation analysis

Taguchi method is not sufficient to optimize more than one output, simultaneously, which can be called as multi-objective optimization. Grey relation analysis (GRA) is used to optimize multi-objective problems. In this study, the multi-objective problem is to find the configuration of the dimple parameters that give highest Nu and lowest f , simultaneously.

The GRA steps consist of main three steps:

1. Normalization of the experimental results
2. Calculation of grey relation coefficients (GRC) of the normalized data
3. Calculation of grey relation grades (GRG)

The normalization criteria as “Higher is better” (Eq. (26)) and “Lower is better” (Eq. (27)) are selected for the Nu and the f , respectively.

The higher is better:

$$x_i^*(k) = \frac{x_i^0(k) - \min x_i^0(k)}{\max x_i^0(k) - \min x_i^0(k)} \tag{26}$$

$$x_i^*(k) = \frac{\max x_i^0(k) - x_i^0(k)}{\max x_i^0(k) - \min x_i^0(k)} \tag{27}$$

Where $x_i^k(k)$ is the normalized value of the k^{th} element in the i^{th} sequence and $\max x_i^0(k)$ and $\min x_i^0(k)$ represent the highest and the lowest value of $x_i^k(k)$. After the normalization, the GRC (ξ_i) is calculated with the following Eqs. (28-31). Δ_{0i} given in Eq. (29) is the absolute value of the difference of the reference sequence ($x_0^*(k)$) and comparable sequence ($x_i^*(k)$). ζ is the distinguish coefficient ranging between 0 and 1, and it is generally used as 0.5 [24], [16], [25], [26], Δ_{min} and Δ_{max} are the lowest and the highest value of Δ_{0i} , respectively.

$$\xi_i(k) = \frac{\Delta_{min} + \zeta \Delta_{max}}{\Delta_{0i}(k) + \zeta \Delta_{max}} \tag{28}$$

$$\Delta_{0i} = \|x_0^*(k) - x_i^*(k)\| \tag{29}$$

$$\Delta_{min} = \min_{j \in i} \min_{\forall k} \|x_0^*(k) - x_j^*(k)\| \tag{30}$$

$$\Delta_{max} = \max_{j \in i} \max_{\forall k} \|x_0^*(k) - x_j^*(k)\| \tag{31}$$

Based on GRC, GRG (γ_i) representing the level of the correlation between the reference sequence and comparability sequence is calculated by Eq. (32).

$$\gamma_i = \frac{1}{n} \sum_{i=1}^n \xi_i(k) \tag{32}$$

3. RESULTS AND DISCUSSIONS

3.1. Validation of the numerical methodology

Comparisons of the results the present study both the smooth tube according to the Nusselt number and the

friction factor are given in Fig. 3. Gnielinski Eq. (33) [27] and Petukhov Eq. (34) [28] are used to compare with the results of the present study according to the Nusselt number and the friction factor, respectively. As can be seen from these figures that a good agreement is obtained between the present study and the literature.

$$Nu = \frac{(f/8)(Re_D-1000)Pr}{1+12.7(f/8)^{1/2}(Pr^{2/3}-1)} \quad (33)$$

$$f = (0.79 \ln(Re) - 1.64)^{-0.2} \quad (34)$$

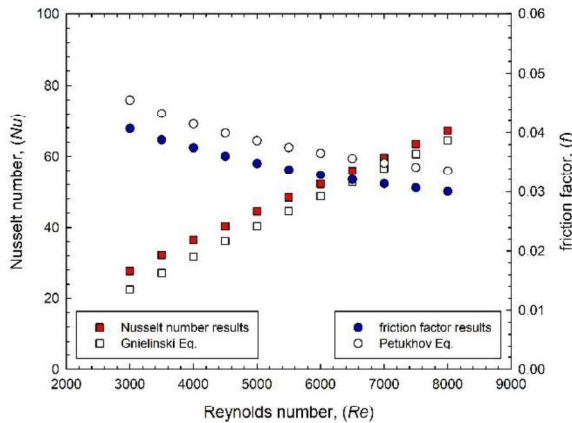


Fig 3. Comparison of results between equations in the literature

3.1. Heat Transfer

3.1.1. Effect of pitch length of the rings

Temperature contours for the cases having various pitch length by holding the inner diameter of 12.5 mm and the thickness of 3.0 mm constant are given in Fig. 4. As observed from the figure that the thermal boundary layer is destructed more significantly as the pitch length of the rings decreasing which led to increase heat transfer through the tube. On the other hand, the decrease in the pitch length of the rings means to the increment of the number of the rings through the test tube. Therefore, the increase in the number of the ring through the tube has a positive role on increase in heat transfer rate.

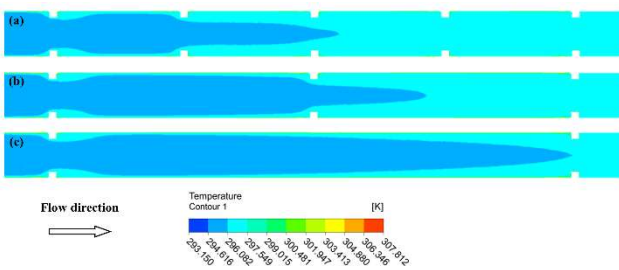


Fig 4. Temperature contours for various pitch length of the rings (a) P=50mm, b) P=100mm and c) P=200mm by holding the inner diameter of 12.5 mm and the thickness of 3 mm.

3.1.2. Effect of inner diameter of the rings

Fig. 5 shows the temperature contours of the cases having various inner diameter of the rings by holding the pitch length of 100 mm and the thickness of 3.0 mm constant.

The decrease in the inner diameter of the rings cause to more thermal boundary layer destruction by preventing the flow. The decrease in the inner diameter of the ring leads to compress the fluid in the core of the tube. As a result, the decrease in the inner diameter of the rings increase the heat transfer rate at behind of the rings.

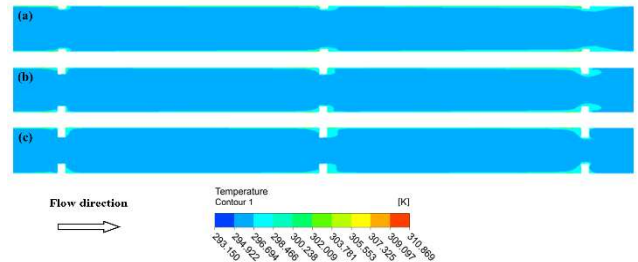


Fig 5. Temperature contours for various inner diameter of the rings (a) d=15.0 mm, b) d=12.5 mm and c) d=10.0 mm) by holding the pitch length of 100 mm and the thickness of 3 mm.

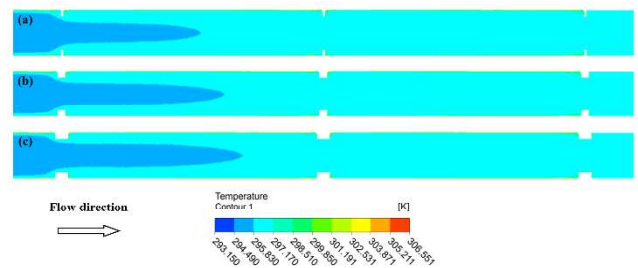


Fig 6. Temperature contours for various thickness of the rings (a) t=1mm, b) t=3mm and c) t=5mm) by holding the inner diameter of 12.5 mm and the pitch length of 100 mm.

3.1.3. Effect of thickness of the rings

Fig. 6 shows the temperature contours of the cases having various thickness of the rings by holding the pitch length of 100 mm and the inner diameter of 12.5 mm constant. The effect of the thickness of the rings for heat exchanger tube inserted with rings can be discussed by examining the figure. The region where there is no flow is much more heated by the heat flux, which lead to heat energy is stored. Furthermore, the length of the flow having low temperature increases with the increment of thickness of the rings. As a result, the thickness of the rings has a positive role on heat transfer enhancement.

3.2. Flow characteristic

3.2.1. Effect of pitch length of the rings

Velocity contours of the cases having various pitch lengths of the rings by holding the inner diameter of 12.5 mm and the thickness of 3 mm are given in Fig. 7. It is expected that the velocity of the fluid which flow in the ring increases due to decrease in cross sectional area of the path. This result is attributed to mass conversation. The rings at the inner wall surface of the tube creates more friction due to pressure drop. An increase the number of used rings through the tube increase the pressure drop directly. Therefore, the decrease in the pitch length increases the friction factor and pressure drop through the tube.

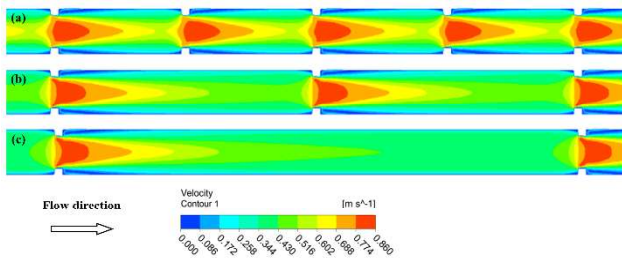


Fig 7. Velocity contours for various pitch length of the rings (a) P=50mm, b) P=100mm and c) P=200mm) by holding the inner diameter of 12.5 mm and the thickness of 3 mm.

3.2.2. Effect of inner diameter of the rings

The decrease in the inner diameter of the ring leads to compress the fluid in the core of the tube which cause to increase velocity. This result can be clearly from the Fig. 8. On the other hand, the decrease in the inner diameter of the ring increases the obstacle surface area through the flow path which cause to pressure drop penalty and so the friction factor.

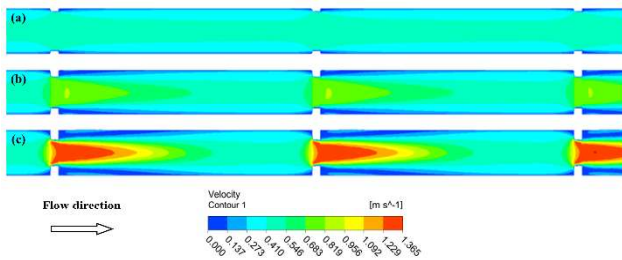


Fig 8. Velocity contours for various inner diameter of the rings (a) d=15.0 mm, b) d=12.5 mm and c) d=10.0 mm) by holding the pitch length of 100 mm and the thickness of 3 mm.

3.2.3. Effect of thickness of the rings

The velocity contour of various thickness of the rings is shown in Fig. 9. As the thickness of the ring increases, the wake region behind the ring increases. Besides, as the length of the flow path inside the ring becomes longer, the velocity magnitude at the regions, where the rings are placed, decreases compared to other counterparts. As a result, it can be stated that the increase in velocity magnitude through the tube cause to increase friction factor.

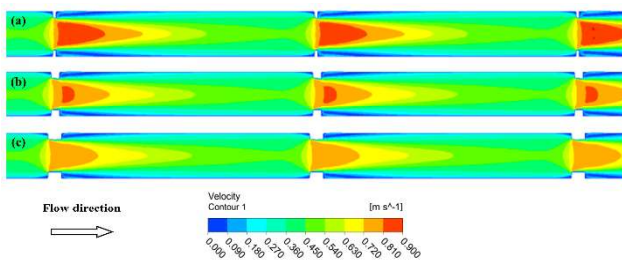


Fig 9. Velocity contours for various thickness of the rings (a) t=1mm, b) t=3mm and c) t=5mm) by holding the inner diameter of 12.5 mm and the pitch length of 100 mm.

3.3. Optimization

The effect of considered heat exchanger tube inserted with rings that are pitch length, inner diameter and thickness of

the rings are discussed according to heat transfer and flow characteristic. An optimum configuration will be revealed at this section according to single and multi-objective optimization techniques.

Table 3 Results obtained by the numerical study and Taguchi method

| Run | Factors | | | Results | | SNR | |
|-----|---------|---|---|---------|--------|--------|--------|
| | P | d | t | Nu | f | Nu | f |
| 1 | 1 | 1 | 1 | 108.18 | 0.1590 | 40.683 | 15.973 |
| 2 | 1 | 2 | 2 | 130.10 | 0.6849 | 42.286 | 3.288 |
| 3 | 1 | 3 | 3 | 171.03 | 2.6893 | 44.662 | -8.593 |
| 4 | 2 | 1 | 2 | 95.10 | 0.0865 | 39.563 | 21.258 |
| 5 | 2 | 2 | 3 | 111.54 | 0.3506 | 40.949 | 9.104 |
| 6 | 2 | 3 | 1 | 144.89 | 1.9904 | 43.221 | -5.979 |
| 7 | 3 | 1 | 3 | 87.81 | 0.0622 | 38.871 | 24.123 |
| 8 | 3 | 2 | 1 | 99.60 | 0.2679 | 39.965 | 11.442 |
| 9 | 3 | 3 | 2 | 115.10 | 0.7872 | 41.221 | 2.079 |

3.3.1. Single-objective optimization

Taguchi method is adopted to reveal an optimum configuration according to heat transfer and flow characteristic identically. The *Nu* and the *f* results are used to evaluate the heat transfer and the flow characteristic of the considered tube, respectively. The SNR (signal to noise ratio) values obtained from the Taguchi method according to the numerical results are given in Table 3.

The average SNR values for the *Nu* are given in Table 4 and plotted in Fig. 10. The optimum configuration is A1B3C3 corresponding to the pitch length of 50 mm, inner diameter of 10.0 mm and thickness of 5 mm according to the *Nu*.

Table 4 Average SNR values for the *Nu*

| Factors | Levels | | |
|-----------------------|--------|-------|--------|
| | 1 | 2 | 3 |
| A: Pitch length (P) | 42.54* | 41.24 | 40.02 |
| B: Inner diameter (d) | 39.71 | 41.07 | 43.03* |
| C: Thickness (t) | 41.29 | 41.02 | 41.49* |
| Mean 41.04 dB. | | | |
| * Optimum level | | | |

The average SNR values for the *f* are given in Table 5 and plotted in Fig. 11. The optimum configuration is A3B1C2 corresponding to the pitch length of 200 mm, inner diameter of 15.0 mm and thickness of 3 mm according to the *f*. This result also can be clearly seen from Fig. 11.

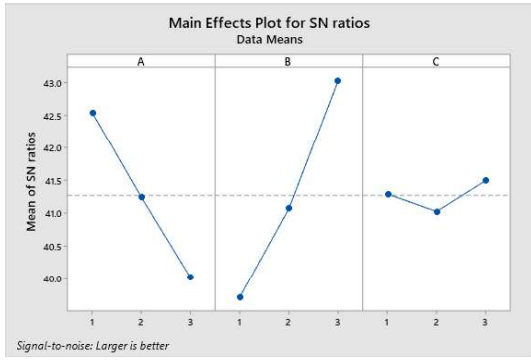


Fig 10. Mean effects plot for SNR for the Nu

Table 5 Average SNR values for the f

| Factors | Levels | | |
|-----------------------|---------|--------|---------|
| | 1 | 2 | 3 |
| A: Pitch length (P) | 3.556 | 8.128 | 12.548* |
| B: Inner diameter (d) | 20.452* | 7.945 | -4.164 |
| C: Thickness (t) | 7.146 | 8.875* | 8.211 |
| Mean 8.077 dB. | | | |
| * Optimum level | | | |

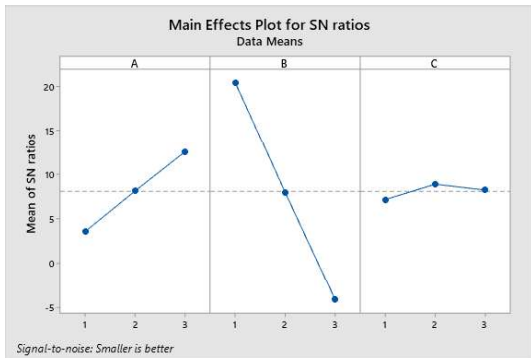


Fig 11. Mean effects plot for SNR for the f

3.3.2. ANOVA

Analysis of variance (ANOVA) study is performed on the SNR results from the Taguchi method to reveal the contribution effect of the factors on the Nu and the f . F-test with confidence level of 95% is used to assess the significance of the considered dimple parameters on the Nu and the f . Table 6 and Table 7 show the ANOVA results for the Nu and the f , respectively. F_{test} value being higher than $F_{0.05}$ indicates that the optimization study is confidence in %95 interval. Thereby, the confidence of the optimization study is ensured in %95 for the factors and for both the Nu and the f . According to Table 6 and Table 7, the most effective factor is inner diameter for both the Nu and the f , with of 61.88% and 87.38%, respectively. Besides, the confidence of the ANOVA is ensured by comparing the F-test value with $F_{0.05}$ values for both the Nu and the f .

Table 6 Average SNR values for the Nu

| Factors | dof | SS | V | F-test | $F_{0.05}$ | Cont. level (%) |
|---------|-----|--------|-------|--------|------------|-----------------|
| P | 2 | 9.5593 | 4.779 | 20.74 | 0.046 | 35.20 |
| d | 2 | 16.805 | 8.402 | 36.46 | 0.027 | 61.88 |
| t | 2 | 0.3336 | 0.166 | 0.72 | 0.580 | 1.23 |
| Error | 2 | 0.4609 | 0.230 | | | 1.70 |
| Total | 8 | | | | | 100 |

Table 7 Average SNR values for the f

| Factors | dof | SS | V | F-test | $F_{0.05}$ | Cont. level (%) |
|---------|-----|---------|--------|--------|------------|-----------------|
| P | 2 | 121.29 | 60.644 | 22.18 | 0.043 | 11.66 |
| d | 2 | 908.99 | 454.49 | 166.21 | 0.006 | 87.38 |
| t | 2 | 4.57 | 2.283 | 0.84 | 0.545 | 0.44 |
| Error | 2 | 5.47 | 2.734 | | | 0.53 |
| Total | 8 | 1040.32 | | | | 100 |

3.3.3. Confirmation test

A confirmation test is performed to check whether the accuracy of the optimization methodology is accurate, or not. Initial parameters indicating the largest SNR value for both Nu and f are firstly selected to show the improvement in the SNR. A1B3C3 and A3B1C3 are selected as the initial parameters for the Nu and the f , respectively. Then, the optimum parameters are predicted for both h and ΔP by using Eq. (17).

$$\hat{\eta} = \eta_m + \sum_{i=1}^p (\hat{\eta}_i - \eta_m) \tag{35}$$

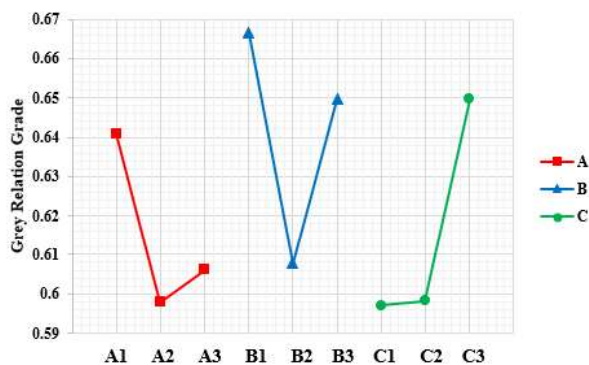
Where, $\hat{\eta}$ is the average of the SNR on the optimum level, η_m is the total average of the SNR and p is the number of parameters affecting the performance. According to confirmation test, it is found that the optimum configuration is also in the DoE. Since the predicted values for the Nu and the f would be same with the optimum values, the optimization methodology is ensured by confirmation test.

3.3.4. Multi-objective optimization

In order to reveal an optimum configuration indicating both the highest Nu and the lowest f , a multi-objective optimization study is performed by using Grey relation analysis (GRA). The obtained results of the GRA for the experiment plan are given in Table 8. According to the Table 8, 4thrun(A2B1C2) present the optimum result which is the highest Nu and the lowest f in the DoE. The general optimum configuration can be apart from the experiment plan. For this scope, the Grey relation grade is generally calculated as plotted in Fig. 12. As read from this figure, the configuration providing the multi-objective optimization is A1B1C3 corresponding to the pitch length of 50 mm, the inner diameter of 15.0 mm and the thickness of 5.0 mm.

Table 8 GRA results for the numerical runs

| Runs | Normalized data | | Deviation sequence | | Grey relation coefficient | | Grey relation grade | Order |
|------|-----------------|-------|--------------------|-------|---------------------------|-------|---------------------|-------|
| | Nu | f | Nu | f | Nu | f | | |
| 1 | 0.245 | 0.963 | 0.755 | 0.037 | 0.398 | 0.931 | 0.665 | 4 |
| 2 | 0.508 | 0.763 | 0.492 | 0.237 | 0.504 | 0.678 | 0.591 | 7 |
| 3 | 1.000 | 0.000 | 0.000 | 1.000 | 1.000 | 0.333 | 0.667 | 2 |
| 4 | 0.088 | 0.991 | 0.912 | 0.009 | 0.354 | 0.982 | 0.668 | 1 |
| 5 | 0.285 | 0.890 | 0.715 | 0.110 | 0.412 | 0.820 | 0.616 | 6 |
| 6 | 0.686 | 0.266 | 0.314 | 0.734 | 0.614 | 0.405 | 0.510 | 9 |
| 7 | 0.000 | 1.000 | 1.000 | 0.000 | 0.333 | 1.000 | 0.667 | 2 |
| 8 | 0.142 | 0.922 | 0.858 | 0.078 | 0.368 | 0.865 | 0.616 | 5 |
| 9 | 0.328 | 0.724 | 0.672 | 0.276 | 0.427 | 0.644 | 0.535 | 8 |

**Fig 12.** Effects of the parameters on multi-objective optimization

4. CONCLUSION

The geometric parameters of a heat exchanger tube inserted with circular rings are numerically investigated and optimized according to the thermal and the hydraulic performance. In order to reduce the number of numerical runs design of experiment (DoE) by Taguchi method is used. The single-objective optimization which finds an optimum configuration is performed by Taguchi method according to the Nu or the f , while multi-objective optimization is performed by GRA according to both the Nu and the f . Besides, ANOVA is conducted to reveal the contribution effects of the factors on the Nu and the f results. The conclusions found from the studies are drawn in the following:

- The Nu and the f increases as the pitch length, the inner diameter and thickness of rings decreases.
- For the single-objective optimization, the highest Nu and the lowest f is obtained with the tube configuration that are A1B3C3 (i.e. the P of 50 mm, the d of 10 mm and the t of 5 mm) and A3B1C2 (i.e. the P of 200 mm, the d of 15 mm and the t of 3.0 mm), respectively.
- The contribution levels of the parameters are of P, d and t are determined for the Nu and the f as 35.20%, 61.88% and 1.23% and 11.66%, 87.38% and 0.44%, respectively.

- A1B1C3 (i.e. the P of 50 mm, the d of 15.0 mm and the t of 5.0 mm) presents the best thermal and hydraulic performance according to the multi-objective optimization study.

REFERENCES

- [1] M. Omidi, M. Farhadi, and M. Jafari, "A comprehensive review on double pipe heat exchangers," *Appl. Therm. Eng.*, vol. 110, pp. 1075–1090, Jan. 2017.
- [2] T. Alam and M.-H. Kim, "A comprehensive review on single phase heat transfer enhancement techniques in heat exchanger applications," *Renew. Sustain. Energy Rev.*, vol. 81, pp. 813–839, Jan. 2018.
- [3] L. Léal *et al.*, "An overview of heat transfer enhancement methods and new perspectives: Focus on active methods using electroactive materials," *Int. J. Heat Mass Transf.*, vol. 61, pp. 505–524, Jun. 2013.
- [4] D. Panahi and K. Zamzamin, "Heat transfer enhancement of shell-and-coiled tube heat exchanger utilizing helical wire turbulator," *Appl. Therm. Eng.*, vol. 115, pp. 607–615, 2017.
- [5] R. K. Shah, "Extended surface heat transfer," in *A-to-Z Guide to Thermodynamics, Heat and Mass Transfer, and Fluids Engineering*, Begellhouse.
- [6] M. Sheikholeslami, M. Gorji-Bandpy, and D. D. Ganji, "Review of heat transfer enhancement methods: Focus on passive methods using swirl flow devices," *Renew. Sustain. Energy Rev.*, vol. 49, pp. 444–469, Sep. 2015.
- [7] M. Uyanik, T. Dagdevir, and V. Ozceyhan, "Thermo-hydraulic performance investigation of a heat exchanger tube inserted with twisted tapes modified with various twist ratio and alternate axis," *Eur. Mech. Sci.*, vol. 6, no. 3, pp. 189–195, Sep. 2022.
- [8] M. M. Ibrahim, M. A. Essa, and N. H. Mostafa, "A computational study of heat transfer analysis for a circular tube with conical ring turbulators," *Int. J. Therm. Sci.*, vol. 137, pp. 138–160, Mar. 2019.
- [9] P. Promvong, "Thermal performance in circular tube fitted with coiled square wires," *Energy Convers. Manag.*, vol. 49, no. 5, pp. 980–987, May 2008.
- [10] P. Promvong, "Heat transfer behaviors in round tube with conical ring inserts," *Energy Convers. Manag.*, vol. 49, no. 1, pp. 8–15, Jan. 2008.
- [11] P. Promvong and S. Eiamsa-ard, "Heat transfer and turbulent flow friction in a circular tube fitted with conical-nozzle turbulators," *Int. Commun. Heat Mass Transf.*, vol. 34, no. 1, pp. 72–82, Jan. 2007.
- [12] P. Promvong and S. Eiamsa-ard, "Heat transfer behaviors in a tube with combined conical-ring and twisted-tape insert," *Int. Commun. Heat Mass Transf.*, vol. 34, no. 7, pp. 849–859, Aug. 2007.
- [13] V. Kongkaiptaiboon, K. Nanan, and S. Eiamsa-ard, "Experimental investigation of convective heat transfer and pressure loss in a round tube fitted with circular-ring turbulators," *Int. Commun. Heat Mass Transf.*, vol. 37, no. 5, pp. 568–574, May 2010.
- [14] M. Mohammadi, A. Abadeh, R. Nemati-Farouji, and M. Passandideh-Fard, "An optimization of heat transfer of nanofluid flow in a helically coiled pipe using Taguchi method," *J. Therm. Anal. Calorim.*, vol. 138, no. 2, pp. 1779–1792, Oct. 2019.
- [15] P. V. K. V. Kola, S. K. Pisipaty, S. S. Mendu,

- and R. Ghosh, "Optimization of performance parameters of a double pipe heat exchanger with cut twisted tapes using CFD and RSM," *Chem. Eng. Process. - Process Intensif.*, vol. 163, p. 108362, Jun. 2021.
- [16] E. Turgut, G. Çakmak, and C. Yıldız, "Optimization of the concentric heat exchanger with injector turbulators by Taguchi method," *Energy Convers. Manag.*, vol. 53, no. 1, pp. 268–275, Jan. 2012.
- [17] S. Chamoli, P. Yu, and A. Kumar, "Multi-response optimization of geometric and flow parameters in a heat exchanger tube with perforated disk inserts by Taguchi grey relational analysis," *Appl. Therm. Eng.*, vol. 103, pp. 1339–1350, Jun. 2016.
- [18] T. Dagdevir, "Multi-objective optimization of geometrical parameters of dimples on a dimpled heat exchanger tube by Taguchi based Grey relation analysis and response surface method," *Int. J. Therm. Sci.*, vol. 173, p. 107365, Mar. 2022.
- [19] E. Dagdevir and M. Tokmakci, "Optimization of preprocessing stage in EEG based BCI systems in terms of accuracy and timing cost," *Biomed. Signal Process. Control*, vol. 67, p. 102548, May 2021.
- [20] T. L. Bergman, A. S. L. and F. P. Incropera, D. P. DeWitt, and A. S. Incropera, F. P., DeWitt, D. P., Bergman, T. L., & Lavine, *Fundamentals of heat and mass transfer*, 6th ed. New York: Wiley, 1996.
- [21] Fluent, "ANSYS Fluent User Guide." New Hampshire, 2016.
- [22] G. Taguchi, *Taguchi Techniques for Quality Engineering*. New York, 1987.
- [23] I. Kotcioglu, A. Cansiz, and M. Nasiri Khalaji, "Experimental investigation for optimization of design parameters in a rectangular duct with plate-fins heat exchanger by Taguchi method," *Appl. Therm. Eng.*, vol. 50, no. 1, pp. 604–613, Jan. 2013.
- [24] N. H. Naqiuddin *et al.*, "Numerical investigation for optimizing segmented micro-channel heat sink by Taguchi-Grey method," *Appl. Energy*, vol. 222, pp. 437–450, Jul. 2018.
- [25] S. Kumar and R. Singh, "Optimization of process parameters of metal inert gas welding with preheating on AISI 1018 mild steel using grey based Taguchi method," *Measurement*, vol. 148, p. 106924, Dec. 2019.
- [26] T. Dagdevir and V. Ozceyhan, "Optimization of process parameters in terms of stabilization and thermal conductivity on water based TiO₂ nanofluid preparation by using Taguchi method and Grey relation analysis," *Int. Commun. Heat Mass Transf.*, p. 105047, Nov. 2020.
- [27] Gnielinski V., "New equations for heat and mass transfer in turbulent pipe and channel flow," *Int. Chem. Eng.*, vol. 27, pp. 359–368, 1976.
- [28] B. S. Petukhov, T. F. Irvine, and J. P. Hartnett, "Advances in heat transfer," *Acad. New York*, vol. 6, pp. 503–564, 1970.